

# Probing topological protected transport in finite-sized Su-Schrieffer-Heeger chains

Yu-Han Chang,<sup>1</sup> Nadia Daniela Rivera Torres,<sup>2</sup> Santiago Figueroa Manrique,<sup>2</sup> Raul A. Robles Robles,<sup>3</sup> Vanna Christmas Silalahi,<sup>1</sup> Cen-Shawn Wu,<sup>4</sup> Gang Wang,<sup>5</sup> Giulia Marcucci,<sup>6,7,8</sup> Laura Pilozzi,<sup>7,9</sup> Claudio Conti,<sup>6,7,9</sup> Ray-Kuang Lee,<sup>2,3,10,11,\*</sup> and Watson Kuo<sup>1,11,†</sup>

<sup>1</sup>*Department of Physics, National Chung Hsing University, Taichung 402, Taiwan*

<sup>2</sup>*Department of Physics, National Tsing Hua University, Hsinchu 300, Taiwan*

<sup>3</sup>*Institute of Photonics Technologies, National Tsing Hua University, Hsinchu 300, Taiwan*

<sup>4</sup>*Department of Physics, National Chang-Hua University of Education, Changhua 500, Taiwan*

<sup>5</sup>*School of Physical Science and Technology, Soochow University, Suzhou 215006, China*

<sup>6</sup>*Department of Physics, University Sapienza, Rome 00185, Italy*

<sup>7</sup>*Institute for Complex Systems, National Research Council (ISC-CNR), Rome 00185, Italy*

<sup>8</sup>*Apho Ltd, 242 Acklam Rd, London W10 5JJ, United Kingdom*

<sup>9</sup>*Research Center Enrico Fermi, Via Panisperna 89a, 00184 Rome, Italy*

<sup>10</sup>*Physics Division, National Center for Theoretical Sciences, Taipei 10617, Taiwan*

<sup>11</sup>*Center for Quantum Technology, Hsinchu 30013, Taiwan*

In order to transport information with topological protection, we reveal and demonstrate experimentally the existence of a characteristic length  $L_c$ , coined as the *transport length*, in the bulk size for edge states in one-dimensional Su-Schrieffer-Heeger (SSH) chains. In spite of the corresponding wavefunction amplitude decays exponentially, characterized by the penetration depth  $\xi$ , the transport between two edge states remains possible even when the lattice size  $L$  is much larger than the penetration depth, i.e.,  $\xi \ll L \leq L_c$ . Due to the non-zero coupling energy in a finite-size system, the supported SSH edge states are not completely isolated at the two ends, giving an abrupt change in the wave localization, manifested through the inverse participation ratio to the lattice size. To verify such a non-exponential scaling factor to the system size, we implement a chain of split-ring resonators and their complementary ones with controllable hopping strengths. By performing the measurements on the group velocity from the transmission spectroscopy of non-trivially topological edge states with pulse excitations, the transport velocity between two edge states is directly observed with the number of lattices up to 20. Along the route to harness topology to protect optical information, our experimental demonstrations provide a crucial guideline for utilizing photonic topological devices.

*Introduction.*—Composited by dimers with staggered hopping amplitudes, a topological phase transition can be revealed in the Su-Schrieffer-Heeger (SSH) model owing to the existence of Zak phase associated with zero Berry curvature [1, 2]. By utilizing the SSH model, people have illustrated the difference between bulk and boundary, chiral symmetry, adiabatic equivalence, topological invariants, and bulk–boundary correspondence [3]. Through the analogy in single-particle Hamiltonian, topologically non-trivial zero or  $\pi$  modes can also be observed in photonic systems, through a periodically setting on the confining potentials [4–8]. With the topologically protected edge states, we can implement new types of lasing modes [9, 10] and optical control [11, 12] even under continuous deformations.

As the edge modes in a one-dimensional (1D) SSH model are zero-dimensional, by definition, they do not have a group velocity. However, for the practical implementation, instead of infinite chains, only a finite number of dimers can be fabricated. Moreover, in order to harness topology to protect optical information [13], a natural question arises on the corresponding transport prop-

erties in the supported non-trivially topological states. It is the common belief that the wavefunctions of supported edge states in a finite-size chain should remain staying localized strongly at their respective boundaries and decay exponentially in the bulk, with a penetration depth  $\xi$  depending on the contrast between coupling strengths. On the contrary, in this *Letter*, we reveal the existence of a transport length  $L_c$  in finite-size SSH chains, which is much larger than the penetration depth, i.e.,  $L_c \gg \xi$ . As long as the system size is smaller than this transport length, one can transport information between two supported edge states with non-trivially topological protection.

By calculating the corresponding inverse participation ratio (IPR), an abrupt change in the wave (de)localization happens at this critical length scale, with the comparison to the exponential scaling factor to the system size from the topologically trivial states. Theoretically, the dependence on the lattice size and the contrast between coupling strengths is also derived for the transport length, see Eq. (3) below. Experimentally, the existence of non-trivially optical topological edge states in a chain of dimers with split-ring resonator (SRR) and its counterpart, the complementary split-ring resonator (CSRR), is illustrated with a proper setting on the intra- and inter-cell coupling strengths between SRRs and CSRRs [14]. By extracting the amplitude and

\*Electronic address: rklee@ee.nthu.edu.tw

†Electronic address: wkuo@phys.nchu.edu.tw

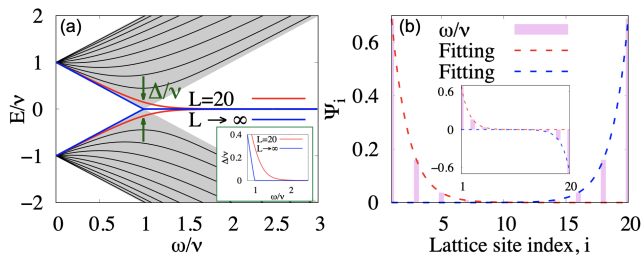


FIG. 1: (a) Energy bands of edge states for finite-size ( $L = 20$ ) and infinite-size ( $L = \infty$ ) SSH models. The coupling energy  $\Delta$  closes ( $\Delta = 0$ ) when  $w/v \geq 1$  only for an infinite-size system. However, for finite-size systems a non-zero value of the energy gap  $\Delta$  occurs even when  $w/v > 1$ , as depicted in the inset. The corresponding edge modes  $\Psi_i$  supported in a finite-size SSH model ( $L = 20$ ) are shown in (b), with the amplitude decaying exponentially, i.e., the fitting dashed-curves of  $\exp[-i/\xi]$  and  $\exp[-(L-i)/\xi]$  with the lattice site index,  $i$ , and the penetration depth  $\xi$ . We want to remark that, instead of the wavefunction pinned to one end, the supported edge state can be symmetric or anti-symmetric combination of the isolated edge modes, as shown in (b) and the inset.

phase from the transmission spectroscopy, a photonic band gap in the passband is measured when the inversion symmetry is broken [15, 16]. The corresponding group velocity of edge states is directly measured with continuous wave and pulse excitations, verifying the transport of edge states when the system size is much larger than the penetration depth. Our results indicate that within this transport length scale the supported edge states possess not only non-trivial topologies, but also a non-exponentially scaling factor in a finite-size SSH model.

*Finite-size SSH chains.*—We consider the SSH model, a 1D tight-binding model with alternating coupling strengths in dimer lattices. In the unit cell of “diatomic basis”, the staggered coupling strengths, denoted as  $v$  and  $w$ , account for the intra- and inter-cells, which lead to a parity effect in the chain length and a gap for the infinite chain case. The SSH model is known for its topological features and shows a transition from a trivial phase to a topological phase as it is tuned crossing  $w/v = 1$ .

When  $w/v \geq 1$ , the normalized energy of edge modes lies at the band center as shown in Fig. 1(a). Outside the band center, one recovers typical Bloch solutions as expected for periodic systems. However, as one can see in Fig. 1(a), the energy gap  $\Delta$  closes ( $\Delta = 0$ ) when  $w/v \geq 1$  only for an infinite-size system. For a finite-size system, such as  $L = 20$  in our experiments, a non-zero value of the energy difference  $\Delta$  occurs for “near-zero” modes even when  $w/v > 1$ , as depicted in the inset of Fig. 1(a). Here,  $L$  denotes the number of lattice sites. Given  $w/v > 1$ ,  $\Delta$  can be approximated by  $\Delta = 2w(\frac{w}{v})^{-N} [1 - (\frac{w}{v})^{-2}] / [1 - (\frac{w}{v})^{-2N}]$  with  $N = L/2$ , the number of unitary cells [17]. Associated with a finite  $\Delta$ , the corresponding modes are no longer isolated

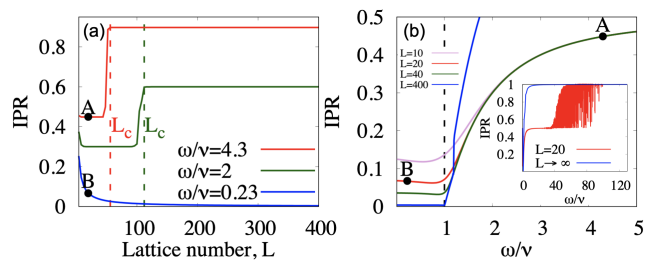


FIG. 2: (a) The Inverse participation ratio (IPR) on the lattice number  $L$  for non-trivial topological states with  $w/v = 2.0$  and  $4.3$ , in green and red colors, respectively. An abrupt change can be identified in the IPR index, marked by the transport length  $L_c$ . As a comparison, in (a) the curve of trivial case with  $w/v = 0.23$  only gives an exponential scaling factor, i.e., the curve in blue color. For a fixed system size  $L = 10, 20, 40$  or  $400$ , in (b) the IPR index is depicted as a function of  $w/v$ , with the large  $w/v$  limit shown in the inset. The markers A and B correspond to our experimental conditions.

at one end, but become a symmetric or anti-symmetric combination of the isolated edge modes, as depicted in Fig. 1(b). In this case,  $\Delta/2$  can be viewed as a coupling energy of the localized modes on each edge, arising from inter-cell coupling  $w$  but scaled exponentially by sample size  $L$ .

Similar to the edge states in an infinite-size system, the wavefunction amplitude of supported edge modes in a finite-size SSH model decays exponentially, characterized by the penetration depth  $\xi = 2/\ln(w/v)$  [17]. As shown in Fig. 1(b), the exponential decaying factors, i.e.,  $\exp[-i/\xi]$  and  $\exp[-(L-i)/\xi]$  with the site label  $i$ , give agreement to the wavefunction amplitudes at both ends. Nevertheless, we want to remark that the penetration length  $\xi$ , independent of the system size  $L$ , is only a few lattice size. In the following, our experiments work at  $w/v = 4.3$ , which gives a penetration length  $2\xi \approx 2.76$  sites.

*Wave localization.*—In order to give a quantitative figure of merit in verifying localization-delocalization transition in these edge states, we calculate the corresponding inverse participation ratio (IPR) index by defining [18],

$$\text{IPR} \equiv \frac{\sum_{i=1}^L |\Psi_i|^4}{(\sum_{i=1}^L |\Psi_i|^2)^2}, \quad (1)$$

which represents a measure of the number of sites contributing to a given state. The clear distinction of IPR index indicates the characteristic features of SSH model, providing a criterion to distinguish the extended (delocalized) states from the localized ones.

Moreover, the IPR index for non-trivial topological states reveals an abrupt change at a characteristic length, denoted as  $L_c$ , as shown in Fig. 2(a). When the system size is smaller than  $L_c$ , the IPR index for the edge modes is small ( $\text{IPR} < 0.5$ ), indicating the existences of

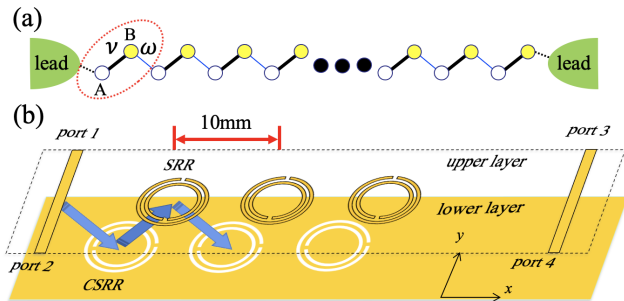


FIG. 3: (a) Schematic of SSH model for 1D microwave propagation in dimer lattices, denoted as  $A$  and  $B$ . The red circle marks the unit cell of “diatomic basis”. (b) The implementation of the SSH model is realized in a finite-size chain by combining split-ring resonator (SRR) and complementary split-ring resonator (CSRR). By varying the orientation of SRR and CSRR, we can manipulate the coupling strengths for the intra- and inter-cells, denoted as  $v$  and  $w$ , respectively. The two leads in the front and end nodes shown in (a) are implemented by two transmission lines in (b), denoted with the input port 1, reflection port 2, and transmissions ports 3 and 4, respectively.

symmetric or anti-symmetric combinations of the edge modes. Specifically, in this regime we have

$$\text{IPR} = \frac{[1 + (\frac{w}{v})^{-2}][1 - (\frac{w}{v})^{-2N}]}{2[1 - (\frac{w}{v})^{-2}][1 + (\frac{w}{v})^{-2N}]} \quad (2)$$

Only when  $L > L_c$ , the IPR index jumps up by a factor of 2, indicating that only strongly isolated states at one side are supported. As a comparison, for all the trivial cases we do not have such an abrupt change in the IPR curve, such as  $w/v = 0.23$  illustrated in Fig. 2(a), which only gives an exponential scaling factor.

As shown in Fig. 2(b), such an abrupt change in the IPR index also exists for a fixed system size when we vary the value of  $w/v$ . For different lattice sizes, such as  $L = 10, 20$ , or  $40$ , the corresponding IPR index curves merge into a single curve; while IPR for  $L = 400$  is doubled when  $w/v$  is sufficiently large.

*Experiments.*—To demonstrate the transport between two edge states even with a lattice size much larger than the penetration depth, as the schematic shown in Fig. 3(a), we fabricate a 1D chain composited by a finite number of sites in the diatomic basis, denoted as  $A$  and  $B$ . The implementation of SSH model is realized by combining SRRs and CSRRs together, but fabricated in the front and back layers, respectively, as illustrated in Fig. 3(b). By bonding these two interleaved layers close enough, with a controllable separation, an effective 1D array can realize the SSH model. In addition to the dimer unit, we manipulate the intra- and inter-cell coupling strengths by varying the orientation of SRRs and CSRRs, respectively.

Regarding the materials, our 1D SSH array is fabricated on the substrate Roger 4003C, which has the thick-

ness 1.6 mm and with copper used as the metallic part of 0.035 mm thickness on it. The resonators are designed with 7.6 mm in diameter, 0.4 mm in line width, along with 0.4 mm between two rings, 0.4 mm for the ring gaps, and 10 mm for the lattice constant. For the  $L = 20$  sample, we have 106.2 mm in total length from the left lead to the right one. It is known that one can manipulate the coupling strengths between SRRs by angle rotations [19–21]. Moreover, for the coupled SRR and CSRR, the texture of orientation produces a great impact on the inter-resonator coupling strength [22]. For a fixed angle of rotation in CSRR, the inter-resonator coupling strength can be varied from 30 MHz to 400 MHz with respect to the angle of rotation in SRR.

Moreover, in order to perform direct measurements on the transmission and reflection spectra, we also introduce two leads in the front and end nodes, as illustrated in Fig. 3(a). With the help of two transmission lines, as shown in Fig. 3(b), here, we define the input (port 1), reflection (port 2), and transmissions ports (3 and 4). To extract the magnitude of coupling strengths in our diatomic cell, simulation results obtained by finite-element simulations are also applied to fit the experimental data, in order to estimate the values of ratio between inter- and intra-cell coupling strengths, i.e.,  $w/v$ .

With the help of experimental parameters extracted from our previous work [22], in the following we demonstrate the direct observation of non-trivial topologically protected edge states for microwave propagation in our 1D chain. Here, an even number of the total lattice sites is fabricated, i.e.,  $L = 20$ , for two sets of orientations of SRR and CSRR at the angles:  $(210^\circ, 290^\circ)$  for non-trivial case and  $(30^\circ, 110^\circ)$  for trivial case, respectively. As the selected angles in these two cases are supplementary, the coupling strengths  $w$  and  $v$  are simply interchanged, with the estimated values of  $w/v = 0.23$  and  $4.3$ , respectively.

*Transmission Spectroscopy.*—In response to directly probe supported non-trivial topologically protected edge states experimentally through the transmission spectroscopy, in Fig. 4(a), we illustrate the calculated transmission spectra  $|T|$  (in dB scale) of 1D SSH model obtained from the theoretical model with non-trivial ( $w/v = 4.3$ ) case for  $L = 20$ , together with the transmission spectrum  $S_{31}$  obtained by direct measurements and finite-element simulations. Non-trivial topological edge states, i.e., the zero-modes, produce the additional resonance peak at gap center ( $\delta = 0$ ). Even though fabrication errors introduce inevitable discrepancy in the measured spectrum, a clear resonant tip can be seen in the transmission spectra, indicating the robustness of topologically protected edge states. On the other hand, transmission spectra in trivial ( $w/v = 0.23$ ) case only presents two passband as in Fig. 4(b).

In addition to the transmission amplitudes, the corresponding phase changes are also shown in Figs. 4(c) and 4(d), for the non-trivial and trivial cases, respectively.

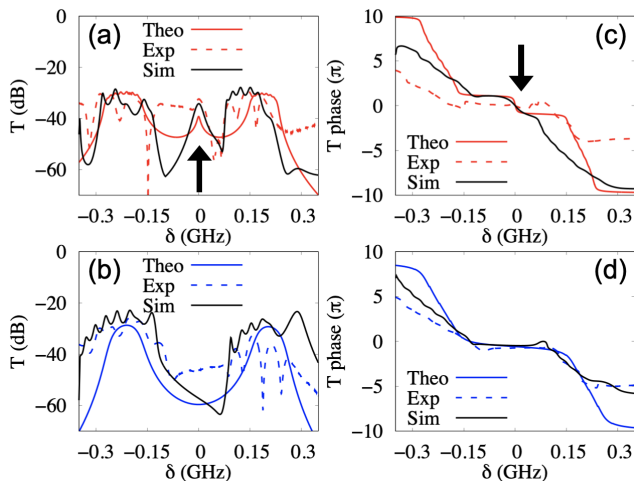


FIG. 4: (a) Transmission spectra  $|T|$  (in dB scale) of 1D SSH model obtained from the theoretical model, experimental measurements and simulations in non-trivial ( $w/v = 4.3$ ) case, while those in trivial case ( $w/v = 0.23$ ) is shown in (b). (c) The corresponding transmission phase (in unit of  $\pi$ ) obtained from the theoretical model, experimental measurements and simulations in non-trivial ( $w/v = 4.3$ ) case; while those in trivial case ( $w/v = 0.23$ ) is shown in (d). The arrows depicted in (a) and (c) indicate the peak and phase shift in the non-trivial case.

One can see that near the zero-detuning region, when  $w/v > 1$ , a phase jump of  $2\pi$  can be clearly identified in Fig. 4(c), for the existence of the non-trivial topologically protected edge state from two Zak phases in  $\pm\pi$  at  $\delta = 0$ . As a comparison no such a phase jump happens for the trivial topological phase, as shown in Fig. 4(d). These transmission spectra clearly demonstrate that our observed states indeed are non-trivial zero modes.

With pulse excitations, depicted in solid-black curves in Figs. 5(a) and (b), we show the direct experimental measurements on the group velocity of supported edge states, for non-trivial case  $w/v = 4.3$  and trivial case  $w/v = 0.23$ , respectively. In addition to the theoretical prediction, a significant dip in the measured group velocity, as well as in the simulated one, can be clearly identified for the non-trivially case, indicating a much lower group velocity than the light speed. Our results give a direct observation of the topologically protected edge states in slow-light, with the measured group velocity  $\sim 13.6 \times 10^6$  m/s. On the contrary, the group velocity of trivial cases propagates at the speed of light in the bulk, i.e.,  $\sim 0.75 \times 10^8$  m/s with the refractive index 4.

In order to manifest the transport property of our supported non-trivial edge states in the finite-size SSH chains, we show the corresponding group velocity on the zero-detuning condition  $\delta = 0$  in Fig. 5(c), as a function of the lattice number  $L$ . As one can see, the group velocity for the non-trivially topological states  $w/v = 4.3$ , depicted in red-color, significantly remains as a constant

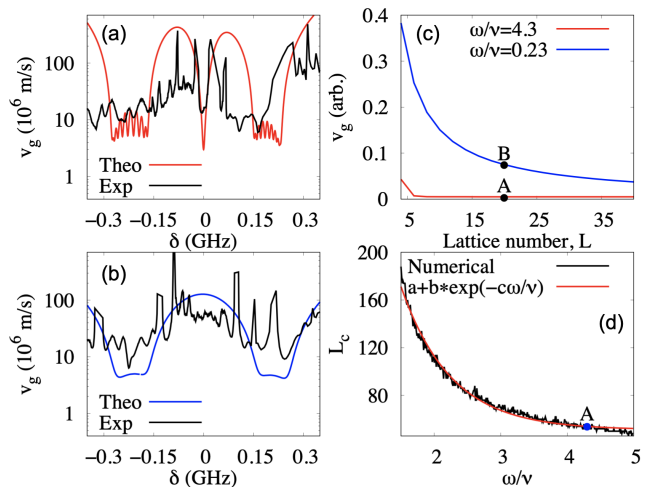


FIG. 5: The measured group velocities for (a) non-trivial case  $w/v = 4.3$  and (b) trivial case  $w/v = 0.23$ , as a function of frequency detuning  $\delta$ . Here, in addition to the theoretical prediction, the experimental measurements are performed by pulse excitations. (c) On the zero-detuning condition  $\delta = 0$ , we depict the group velocity as a function of the lattice number  $L$ . One can see that the group velocity for non-trivially topological states  $w/v = 4.3$ , depicted in red-color, significantly remains as a constant when the system size is smaller than the characteristic length, i.e.,  $L < L_c$ . However, the group velocity for the non-trivially topological states  $w/v = 0.23$ , depicted in blue-color, decays exponentially to the system size. The characteristic length  $L_c$  as a function of  $w/v$  is also depicted in (d). The marker A corresponds to our experimental conditions.

when the system size is smaller than the characteristic length, i.e.,  $L < L_c$ . As a comparison, the group velocity for the trivially topological states  $w/v = 0.23$ , depicted in blue-color, is exponentially decaying to the system size.

With the introduction of this characteristic length  $L_c$ , in Fig. 5(d) we provide a guideline on the maximum system size allowed to transport the edge states in the SSH model. Unlike the penetration depth  $\xi$ , the characteristic length  $L_c$  revealed here is much larger than  $\xi$ . Counter-intuitively, as long as the system size is small than  $L_c$ , the transport between two edge modes is allowed even for a system with its size much larger than the penetration length  $L \gg \xi$ . For a better understanding its origin,  $L_c$  is associated with a threshold in the coupling energy given by  $\frac{\Delta}{v}(L_c) = 10^{-16}$ . From the expression of the energy gap  $\Delta$ , empirically, one finds that:

$$L_c = 2 \frac{\ln(10^{16}) + \ln\left[\frac{w}{\left(\frac{w}{v}\right)^2 - 1}\right]}{\ln\left(\frac{w}{v}\right)}. \quad (3)$$

In more practical situations, disorder or dissipation may attribute to the transport threshold such that  $\Delta(L_c) \sim E_{th}$ , in which  $E_{th}$  is disorder strength or relaxation rate [23].

*Conclusion.*—On the contrary to the common belief that

the wavefunctions of supported edge states in a finite-size chain should decay exponentially in the bulk, we reveal the existence of a transport length in the bulk size for edge states in 1D SSH chains, which is much larger than the penetration depth of the edge modes. A non-exponential scaling factor to the system size is demonstrated though an abrupt change in the wave localization, indicating a possible phase transition for the topological edge states in a finite-size SSH chain. Regarding experimental demonstrations, we implement a chain of interleaved split-ring resonators and complementary split ring resonators with a proper setting in the orientation texture. The existence of non-trivially topological edge states, which are zero modes, is not only demonstrated through the transmission spectra, but also verified through the observation of a  $2\pi$  phase jump. With the non-zero coupling energy in a finite-size system, the group velocity of microwave propagation is directly measured through pulse excitations, revealing a very slow group velocity, down to  $\sim 0.01$  of light speed in free space. The transport length revealed and verified in our experiments provides a crucial guideline for utilizing photonic topological devices, which demonstrates the possibility

to transport optical information with topological protection [24–28].

### Acknowledgement

We are grateful to the National Center for High-performance Computing for computer time and facilities. Fruitful discussions with C. C. Huang and W. H. Chang are acknowledged. G.W. acknowledges the financial supports from National Natural Science Foundation of China (11604231); Natural Science Foundation of Jiangsu Province (BK20160303). This work is financially supported by the Ministry of Science and Technology, Taiwan under grant Nos.106-2112-M-005-007, 108-2923-M-007-001-MY3 and No. 109-2112-M-007-019-MY3), Office of Naval Research Global, US Army Research Office, and Research Center for Sustainable Energy and Nanotechnology, NCHU. This work was co-funded by European Union - PON Ricerca e Innovazione 2014-2020 FESR/FSC - Project ARS01.00734 QUANCOM.

- 
- [1] W. P. Su, J. R. Schrieffer, and A. J. Heeger, “Soliton excitations in polyacetylene,” *Phys. Rev. B* **22**, 2099 (1980).
- [2] A. J. Heeger, S. Kivelson, J. R. Schrieffer, and W. P. Su, “Solitons in conducting polymers,” *Rev. Mod. Phys.* **60**, 781 (1988).
- [3] J. K. Asboth, L. Oroszlany, and A. Palyi, “The Su-Schrieffer-Heeger (SSH) Model,” in *A Short Course on Topological Insulators*, Lecture Notes in Physics, vol. 919 (Springer, 2016).
- [4] N. Malkova, I. Hromada, X. Wang, G. Bryant, and Z. Chen, “Observation of optical Shockley-like surface states in photonic superlattices,” *Opt. Lett.* **34**, 1633 (2009).
- [5] A. B. Khanikaev, S. H. Mousavi, W.-K. Tse, M. Kargarian, A. H. MacDonald, and G. Shvets, “Photonic topological insulators,” *Nature Mat.* **12**, 233 (2013).
- [6] L. Lu, J. D. Joannopoulos, and M. Soljacic, “Topological photonics,” *Nature Photon.* **8**, 821 (2014).
- [7] M. C. Rechtsman, J. M. Zeuner, Y. Plotnik, Y. Lumer, D. Podolsky, F. Dreisow, S. Nolte, M. Segev, and A. Szameit, “Two-dimensional topological photonics,” *Nature* **496**, 196 (2013).
- [8] Q. Cheng, Y. Pan, H. Wang, C. Zhang, D. Yu, A. Gover, H. Zhang, T. Li, L. Zhou, and S. Zhu, “Observation of Anomalous  $\pi$  Modes in Photonic Floquet Engineering,” *Phys. Rev. Lett.* **122**, 173901 (2019).
- [9] L. Piloizzi and C. Conti “Topological lasing in resonant photonic structures” *Phys. Rev. B* **93**, 195317 (2016).
- [10] M. Parto, S. Wittek, H. Hodaei, G. Harari, M. A. Bandres, J. Ren, M. C. Rechtsman, M. Segev, D. N. Christodoulides, and M. Khajavikhan, “Edge-Mode Lasing in 1D Topological Active Arrays,” *Phys. Rev. Lett.* **120**, 113901 (2018).
- [11] G. Marcucci, D. Pierangeli, A. J. Agranat, R.-K. Lee, E. DelRe, and C. Conti, “Topological control of extreme waves,” *Nature Comm.* **10**, 5090 (2019).
- [12] S. Xia, D. Jukić, N. Wang, D. Smirnova, L. Smirnov, L. Tang, D. Song, A. Szameit, D. Leykam, J. Xu, Z. Chen, and H. Buljan, “Nontrivial coupling of light into a defect: the interplay of nonlinearity and topology,” *Light: Sci. & Appl.* **9**, 147 (2020).
- [13] T. Dai, Y. Ao, J. Bao, J. Mao, Y. Chi, Z. Fu, Y. You, X. Chen, C. Zhai, B. Tang, Y. Yang, Z. Li, L. Yuan, F. Gao, X. Lin, M. G. Thompson, J. L. O’Brien, Y. Li, X. Hu, Q. Gong, and J. Wang, “Topologically protected quantum entanglement emitters,” *Nature Photon.* **16**, 248 (2022).
- [14] F. Falcone, T. Lopetegi, M. A. G. Laso, J. D. Baena, J. Bonache, M. Beruete, R. Marqués, F. Martín, and M. Sorolla, “Babinet Principle Applied to the Design of Metasurfaces and Metamaterials,” *Phys. Rev. Lett.* **93**, 197401 (2004).
- [15] R. A. Shelby, D. R. Smith, and S. Schultz, “Experimental verification of a negative index of refraction,” *Science* **292**, 77 (2001).
- [16] S. Linden, C. Enkrich, M. Wegener, J. Zhou, T. Koschny, and C. M. Soukoulis, “Magnetic Response of Metamaterials at 100 Terahertz,” *Science* **306**, 1351 (2004).
- [17] N. K. Efremidis, “Topological photonic Su-Schrieffer-Heeger-type coupler,” *Phys. Rev. A* **104**, 053531 (2021).
- [18] B. Kramer and A. MacKinnon, “Localization: theory and experiment,” *Rep. Prog. Phys.* **56**, 1469 (1993).
- [19] I. Sersic, M. Frimmer, E. Verhagen, and A. F. Koenderink, “Electric and Magnetic Dipole Coupling in Near-Infrared Split-Ring Metamaterial Arrays,” *Phys. Rev. Lett.* **103**, 213902 (2009).
- [20] S. S. Seetharaman, C. G. King, I. R. Hooper, and W. L. Barnes, “Electromagnetic interactions in a pair of coupled split-ring resonators,” *Phys. Rev. A* **96**, 085426 (2017).

- [21] J. Jiang, Z. Guo, Y. Ding, Y. Sun, Y. Li, H. Jiang, and H. Chen “Experimental demonstration of the robust edge states in a split-ring-resonator chain,” *Opt. Exp.* **26**, 12891 (2018).
- [22] Y.-J. Lin, Y.-H. Chang, W.-C. Chien, and W. Kuo, “Transmission line metamaterials based on strongly coupled split ring/complementary split ring resonators,” *Opt. Exp.* **25**, 30395 (2017).
- [23] A. J. Leggett, S. Chakravarty, A. T. Dorsey, M. P. A. Fisher, A. Garg, and W. Zwerger, “Dynamics of the dissipative two-state system,” *Rev. Mod. Phys.* **59**, 1 (1987).
- [24] S. Mittal, J. Fan, S. Faez, A. Migdall, J. M. Taylor, and M. Hafezi, “Topologically Robust Transport of Photons in a Synthetic Gauge Field,” *Phys. Rev. Lett.* **113**, 087403 (2014).
- [25] A. Blanco-Redondo, I. Andonegui, M. J. Collins, G. Harari, Y. Lumer, M. C. Rechtsman, Be. J. Eggleton, and M. Segev, “Topological Optical Waveguiding in Silicon and the Transition between Topological and Trivial Defect States,” *Phys. Rev. Lett.* **116**, 163901 (2016).
- [26] S. Weimann, M. Kremer, Y. Plotnik, Y. Lumer, S. Nolte, K. G. Makris, M. Segev, M. C. Rechtsman and A. Szameit, “Topologically protected bound states in photonic parity–time-symmetric crystals,” *Nature Mat.* **16**, 433 (2017).
- [27] M. Mirhosseini, E. Kim, V. S. Ferreira, M. Kalaei, A. Sipahigil, A. J. Keller and O. Painter, “Superconducting metamaterials for waveguide quantum electrodynamics,” *Nature Comm.* **9**, 3706 (2018).
- [28] G. Arregui, J. Gomis-Bresco, C. M. Sotomayor-Torres, and P. D. Garcia, “Quantifying the Robustness of Topological Slow Light.” *Phys. Rev. Lett.* **126**, 027403 (2021).